Gallium Arsenide Optical Phased Array Beam Steering Photonic Integrated Circuit

Michael Nickerson[1*], Jim Brookhyser[2], Gregory Erwin[2], Bowen Song[1], Jan Kleinert[2], and Jonathan Klamkin[1]
[1]*Department of Electrical and Computer Engineering, University of California, Santa Barbara, CA 93106, USA*
[2]*MKS Instruments, Photonics Solutions Division, 14523 SW Millikan Way, Beaverton, OR 97005, USA*
**nickersonm@ece.ucsb.edu*

Abstract: A 16-channel optical phased array is fabricated on a gallium arsenide photonic integrated circuit platform for operation near 1064 nanometers. The array demonstrates 0.92° beamwidth, 15.3° grating-lobe-free steering range, and 12 dB sidelobe suppression. © 2023 The Author(s)

1. Introduction

Optical phased arrays (OPAs) are a promising solution for solid-state beam steering, with applications ranging from terrestrial navigation LiDAR [1] to free-space optical communication and climate monitoring [2]. Photonic integrated circuit (PIC) technology provides a path to scale OPA channel count and beam size. Existing OPA PIC research has focused on silicon photonics and lithium niobate operating near 1550 nm [3], but practical systems remain challenging due to the lack of native gain and efficient phase modulators with low residual amplitude modulation (RAM). Silicon is also limited to wavelengths greater than 1100 nm, excluding wavelengths commonly utilized by topographical and remote sensing LiDAR. In contrast, group III-V semiconductor platforms offer native optical gain and efficient low-RAM phase modulators across a wide wavelength range.

In this work, a gallium arsenide (GaAs) PIC platform was demonstrated and leveraged to realize an integrated OPA with low fabrication complexity and broadband, high speed, low-RAM phase modulators. The OPA achieved a 0.92° beamwidth, 15.3° grating-lobe-free steering range, and 12 dB sidelobe suppression at an operating wavelength of 1064 nm. Engineered for simple integration of GaAs-based lasers [4], this PIC demonstrates the platform's suitability for monolithically integrated and scalable OPAs.

2. Design, Fabrication, and Integration

Figure 1(a) shows a fabricated PIC with a footprint of 5.2 mm × 1.2 mm. The OPA has a single 5-µm-wide cleaved facet input waveguide which then tapers to a width of 2 µm. This waveguide then splits into 16 equal channels via a cascaded tree of 1×2 multi-mode interference (MMI) couplers. Each channel comprises identical 3-mm-long and 2-µm-wide phase modulators, and then all channels are routed to a 4-µm-pitch cleaved-facet OPA output.

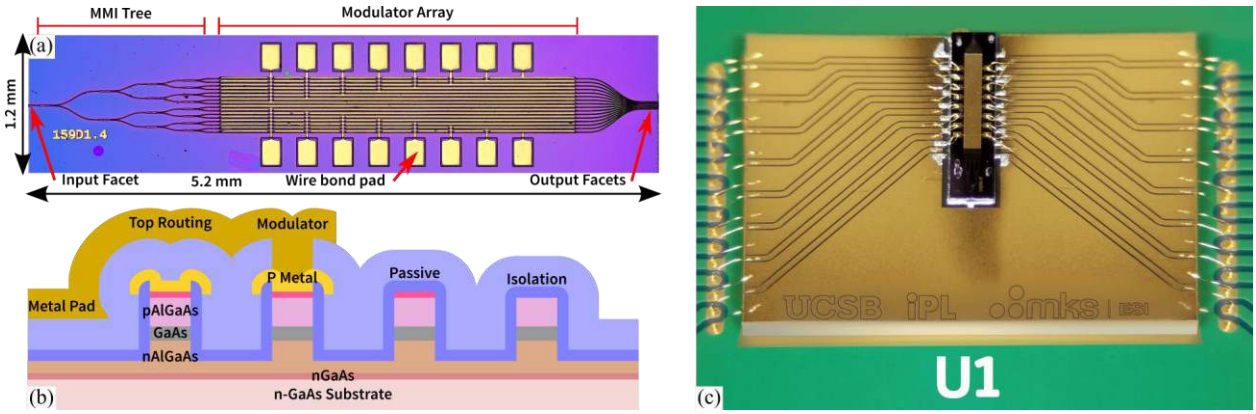

Figure 1. (a) Optical micrograph of fabricated PIC. (b) Simplified cross-section schematic of integrated components. (c) Photograph of PIC mounted on carrier and PCB, retouched for clarity.

The design of the epitaxial structure is based on a previously reported P-p-i-n-N double heterostructure optimized for phase modulation [5]. PIC components were physically implemented with deeply etched ridge waveguides formed by chlorine-based dry etching (Figure 1(b)). P-contacts were formed on top of the phase modulator ridge waveguides. The PIC was isolated with thick dielectric material. Vias were opened to expose the P-contact metal, and trace and wire bonding metal was deposited. Segments of the top p-type material were removed to provide longitudinal electrical isolation. After substrate thinning, a common N-contact was formed on the back side of the n-doped GaAs substrate.

After fabrication, PICs were facet cleaved, AR coated, and then singulated. PICs were soldered and wire bonded to carriers, and the carriers were soldered and wire bonded to printed circuit boards (PCBs) as shown in Figure 1(c).

3. Experimental Beam Steering Results

Phase modulation efficiency was characterized by fitting single-sided Mach-Zehnder modulator transmission measurement results. Modulator electro-optical performance was characterized by measuring the far-field power variation due to single-element electrical modulation. Results at 1030 nm were similar to those previously reported [5], with single-sided $V_\pi \cdot L$ efficiency of 0.7 V·cm, RAM below 0.5 dB for greater than 4π phase modulation, DC power consumption less than 5 μW at 2π phase modulation, and greater than 770 MHz electro-optical bandwidth.

OPA performance was evaluated by coupling light from a 1064 nm laser through a lensed fiber. The OPA output was collected with a 4-mm effective focal length (EFL) objective lens, reimaged with a 500-mm EFL relay lens to a 500-μm effective emitter spacing, and then propagated to the far field and recollimated with a 1147-mm EFL lens onto an Ophir LT665 beam profiling camera.

Figure 2(a) shows the measured beam profile at 0° steering compared to the simulated performance. The measured beamwidth was 0.92°, the grating-lobe-free steering range was 15.3°, and the sidelobe level (SLL) was 12 dB, differing from simulation by only 8%, 0.7%, and 1 dB respectively. By capturing beam profiles across the steering range, the OPA demonstrated an output profile that reproduced the expected envelope, as shown in Figure 2(b), and maintained performance across the entire grating-lobe-free steering range with 0.93° ± 0.01° beamwidth and 12.1 ± 0.4 dB SLL, as shown in Figure 2(c).

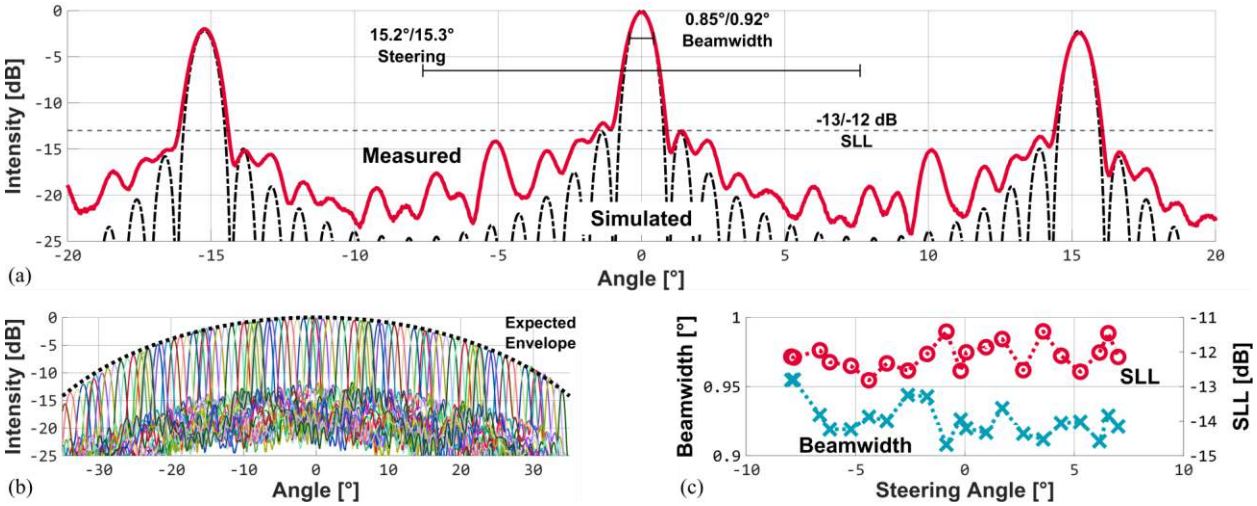

Figure 2. (a) Simulated (black, dashed) and measured (red, solid) beam profiles with indicated simulated/measured beam width, steering range, and sidelobe level. (b) Measured beam profiles at 21 different steering angles (solid), compared to expected envelope (dotted). (c) Beamwidth (left, crosses) and sidelobe level (right, circles) at measured steering angles.

4. Conclusion

A 16-channel GaAs OPA demonstrated a 0.92° beamwidth, a 15.3° grating-lobe-free steering range, and a 12 dB SLL at 1064 nm, all of which were in close agreement with theoretical results. This PIC demonstrates the feasibility for GaAs to realize monolithically integrated and scalable OPAs for beam steering applications.

5. Acknowledgements

The authors acknowledge funding support from MKS Instruments. A portion of this work was performed in the UCSB Nanofabrication Facility, an open access laboratory.

6. References

[1] S. Royo and M. Ballesta-Garcia, "An Overview of Lidar Imaging Systems for Autonomous Vehicles," *Applied Sciences*, vol. 9, no. 19, p. 4093, 19, Multidisciplinary Digital Publishing Institute, Jan. 2019. https://doi.org/10.3390/app9194093

[2] J. Fridlander *et al.*, "Dual Laser Indium Phosphide Photonic Integrated Circuit for Integrated Path Differential Absorption Lidar," *IEEE Journal of Selected Topics in Quantum Electronics*, vol. 28, no. 1, pp. 1–8, Jan. 2022. https://doi.org/10/gmzfnf

[3] M. Zhang, C. Wang, P. Kharel, D. Zhu, and M. Lončar, "Integrated lithium niobate electro-optic modulators: when performance meets scalability," *Optica, OPTICA*, vol. 8, no. 5, pp. 652–667, Optical Society of America, May 2021. https://doi.org/10/gj47x3

[4] P. A. Verrinder *et al.*, "Gallium Arsenide Photonic Integrated Circuit Platform for Tunable Laser Applications," *IEEE Journal of Selected Topics in Quantum Electronics*, vol. 28, no. 1: Semiconductor Lasers, pp. 1–9, Jan. 2022. https://doi.org/10/gmzfnn

[5] M. Nickerson, P. Verrinder, L. Wang, B. Song, and J. Klamkin, "Broadband Optical Phase Modulator with Low Residual Amplitude Modulation," *Optica Advanced Photonics Congress 2022 (2022), paper IW4B.4*, Jul. 24, 2022. https://doi.org/10/grtvck